Full three-body primitive semiclassical treatment of H_2^+

Karl Sohlberg, Robert E. Tuzun, Bobby G. Sumpter, and Donald W. Noid
Chemical and Analytical Sciences Division 4500N MS6197, Oak Ridge National Laboratory, Oak Ridge, Tennessee 37831
(Received 18 August 1997; revised manuscript received 26 September 1997)

Primitive semiclassical quantization of H_2^+ and D_2^+ without the restriction of the separation of electronic and nuclear motions, reveals the existence of a small (10%) classical contribution to the one-electron chemical bond. It is found that in the electronic ground state the electron is exchanged classically between the two nuclei and that this exchange is correlated with the molecular vibration. [S1050-2947(98)03302-2]

PACS number(s): 31.10.+z, 31.15.Gy

I. INTRODUCTION

Very shortly after its inception, Schrödinger's wave mechanics was successfully applied to the hydrogen molecular ion H_2^+ [1]. Numerous earlier attempts to derive the structure of the hydrogen molecular ion in terms of the old quantum theory had failed. The unqualified success of the wave mechanics on this and other molecular systems therefore led Pauling to note [1] the following:

''It is of particular significance that the straightforward application of the quantum mechanics results in the unambiguous conclusion that two hydrogen atoms will form a molecule but that two helium atoms will not; for this distinction is characteristically chemical, and its clarification marks the genesis of the science of sub-atomic theoretical chemistry.''

From that time on, chemical bonding has been viewed as a quantum-mechanical phenomenon, a view now entrenched in the textbook literature of physical chemistry [2]. A few subtle apparent contradictions to Pauling's declaration are themselves a consequence of tunneling, which is a strictly quantum mechanical phenomenon. Strand and Reinhardt [3], for example, demonstrated that semiclassical methods can be used to recover the chemical bond in H_2^+, provided tunneling is properly accounted for within the semiclassical framework. More recently, the experimental observation [4] of the helium dimer He_2 has demonstrated that two helium atoms can indeed form a ''molecule,'' albeit an extremely fragile one. The bonding in He_2 has subsequently been shown to involve deep penetration of the electron into the classically forbidden region [5].

Müller *et al.* [6] have reported that when the restriction of the separation of electronic and nuclear motions (used by Strand and Reinhardt [3]) is removed, orbits exist in H_2^+ in which the electron is exchanged *classically* between the protons. In the current paper, primitive semiclassical quantization of H_2^+ is employed, without the restriction of the separation of electronic and nuclear motions. These calculations demonstrate that such trajectories result in a small (10%) classical contribution to the chemical bonding in H_2^+. In retrospect then, historical applications of the old quantum theory failed to quantitatively recover the magnitude of the chemical bond in H_2^+ because chemical bonding is a quantum mechanical phenomena, but produced the wrong sign for the binding energy in H_2^+ due only to a lack of modern numerical computing facilities. To date, the full three-body Coulomb problem has yet to succumb to an exact analytical analysis [7] and its accurate description demands a numerical treatment not possible *ante* high speed digital computers.

II. SEMICLASSICAL METHODOLOGY

Semiclassical mechanics allows one to extract approximate quantum eigenenergies from a classical description of the system, in the spirit of the old quantum theory and the WKB approximation [8]. The quantization conditions for a multidimensional system (as discussed in detail by Keller [9] and later by Marcus [10]) are given by

$$\oint_{c_i} \sum_r p_r dq_r = h\left(n_r + \frac{m_r}{4}\right), \tag{1}$$

where the c_i are topologically independent closed paths in configuration space, h is the Planck constant of action, and n and m are integers. The integer m is the Maslov index, which depends on the frequency with which the path touches a caustic, and the integer n is the quantum number. At the heart of semiclassical quantization then is the computation of the action integrals

$$\oint = \mathbf{p}\, d\mathbf{q} = \oint \sum_r p_r dq_r . \tag{2}$$

In the present case, as detailed below, we have chosen to use the surface-of-section (SOS) method of semiclassical quantization [11]. Originally presented for a two-dimensional, nonresonant, quasiperiodic, Hamiltonian system [11], the SOS method has been generalized, first for application to a system with a zero-order 1:1 resonance [12], and then to systems of three dimensions [13,14].

In the SOS method, the topologically independent paths of integration are taken to lie along Poincaré surfaces of section. For an N-dimensional system, given the N coordinates q_r and conjugate momenta p_r, A Poincaré surface of section consists of the set of points (p_r, q_r) where a dynamical trajectory intersects the surface $(q_i = \text{const}\ \forall\ i \neq r)$, subject to $(p_i \geqslant 0\ \forall\ i \neq r)$. (Different branches can be chosen by selecting different signs of the p_i where $i \neq r$.) The quantum condition for such a path then reduces to a one-dimensional integral

$$\oint p_r dq_r = h\left(n_r + \frac{m_r}{4}\right). \tag{3}$$

This reduction in dimensionality is a tremendous simplification and arises because the condition ($q_i = \text{const}\ \forall\ i \neq r$) implies that $dq_i = 0$ everywhere along the path of integration, which forces all terms in the sum (2) to be rigorously zero, save one. A SOS can be generated for each (p_r, q_r) sheet to specify each of the quantum conditions in turn.

A. Choice of the SOS method

At this juncture it is appropriate to comment on other methods of semiclassical quantization and their applicability to the present problem, approximating the eigenstates of H_2^+.

The popular periodic orbit method of Gutzwiller [15] generates the quantum density of states from a knowledge of the periodic classical orbits. It is equally applicable to separable and nonseparable cases. Miller has argued that the periodic orbit method makes approximations beyond the semiclassical approximation [16], an issue that has been resolved, in large measure, by Berry and Tabor [17] through the use of complex periodic orbits. The challenge of locating all of the important periodic orbits precludes the use of this method in the present case.

The Fourier method, based on the work of Percival [18], relies on the computation of the action integrals from the coefficients in a Fourier series representation of the classical coordinates and momenta [19]. The Fourier method has seen considerable success, particularly in the determination of the vibrational levels of coupled oscillator systems [20–22]. Nevertheless, the Fourier method is likely to be prohibitive to use in the current case because it requires that the classical trajectory be numerically integrated for a minimum of several periods of the lowest frequency fundamental mode of the system. In H_2^+, the electronic and nuclear motions differ in their characteristic frequencies by more than two orders of magnitude. This means that in order to successfully apply the Fourier method, it would be necessary to compute trajectories long enough to encompass several periods of the nuclear vibration, but with a step size small enough to track the electronic motion accurately, a prohibitive computational task. The electronic motion is particularly difficult to track with accuracy near the sharp inner turning points, which result from close electron-proton encounters. Such encounters occur frequently on the time scale of the electronic motion.

The adiabatic switching (AS) method, in which a solvable zero-order Hamiltonian is gradually perturbed into the full Hamiltonian over the course of a numerical classical trajectory [23], is not applicable to the ground state of H_2^+ due to the lack of a good zero-order Hamiltonian. The excited σ^* state of H_2^+ in many ways resembles a perturbed hydrogen atom, however, and might be a candidate for investigation with AS. Herein we consider both the electronic ground state of H_2^+ and the σ^* state.

Another method that is particularly appealing for nonseparable coupled oscillator systems is to quantize on a separable Hamiltonian that approximates the fully nonseparable Hamiltonian. An iterative scheme for developing such an approximate Hamiltonian was originally developed by Birkhoff [24] for zero-order nonresonant systems. Extensions have been made to zero-order resonant systems, first with numerical techniques [25], and later analytically [26,27]. The issues of convergence [28] and symmetry [29] have also been addressed. For the present case of H_2^+ the method of approximate Hamiltonians suffers, as does AS, from the lack of a good zero-order Hamiltonian.

The SOS method uses only the full Hamiltonian, and does not require a ''nearby'' zero-order Hamiltonian. Semiclassical quantization on the novel adiabatic invariant of Müller *et al.* [6] is also plausible, and may be more precise, but the insights afforded by the trajectory based nature of the SOS method would be lost.

B. Computational details

The classical Hamiltonian for H_2^+ and its isotopomers is

$$H = \frac{\mathbf{p}_1^2}{2m_1} + \frac{\mathbf{p}_2^2}{2m_2} + \frac{\mathbf{p}_3^2}{2m_3} + \frac{1}{R} - \frac{1}{r_a} - \frac{1}{r_b}, \tag{4}$$

where m_1, m_2, and m_3 are the masses of the two nuclei and the electron, respectively, with coordinates $\mathbf{q}_i$ and momenta and $\mathbf{p}_i$. The distance parameters r_a, r_b, and R are given by

$$\begin{aligned} R &= [(\mathbf{q}_2 - \mathbf{q}_1)\cdot(\mathbf{q}_2 - \mathbf{q}_1)]^{(1/2)}, \\ r_a &= [(\mathbf{q}_3 - \mathbf{q}_1)\cdot(\mathbf{q}_3 - \mathbf{q}_1)]^{(1/2)}, \\ r_b &= [(\mathbf{q}_3 - \mathbf{q}_2)\cdot(\mathbf{q}_3 - \mathbf{q}_2)]^{(1/2)}. \end{aligned} \tag{5}$$

Classical trajectories are represented discretely by numerical solution [30] of the Hamilton differential equations of motion

$$\begin{aligned} (dq_\alpha/dt) &= \frac{\partial H}{\partial p_\alpha}, \\ -(dp_\alpha/dt) &= \frac{\partial H}{\partial q_\alpha}, \end{aligned} \tag{6}$$

using Cartesian coordinates q_α and momenta p_α, where the index α runs over the three spatial coordinates and each of the three particles.

During numerical integration, near one of the previously mentioned close electron-proton encounters, the force between the two particles becomes very large and hence the electron, owing to its small mass, is given tremendous acceleration. If such an encounter is too close, the force exceeds the dynamic range of the numerical integration and conservation of total energy is lost. The calculations reported herein were run, at a minimum, in double (64 bit) precision, but for some trajectories it was necessary to employ quadruple (128 bit) precision to properly track the electron motion [31].

While the trajectories are computed in Cartesian coordinates, these are not the most useful coordinates for semiclassical quantization with the SOS method. We note that in the clamped nuclei approximation, the problem is separable in confocal elliptic coordinates [3,32],

$$\zeta=\frac{(r_a+r_b)}{2C},$$
$$\eta=\frac{(r_a-r_b)}{2C}, \tag{7}$$

where $2C$ is the separation of the foci. We will make certain restrictions on the H_2^+ system that permit the use of a simple extension of the confocal elliptic coordinate system. All three particles are restricted to lie in the (x,y) plane, which is coplanar with the (ζ,η) plane. The foci are at $\pm C$ along the x axis. Additionally, the system is translated to have its center of mass at the $(x,y)=(0,0)$ origin and the total linear momentum of the system is zero,

$$\mathbf{P}=\mathbf{p}_1+\mathbf{p}_2+\mathbf{p}_3=0. \tag{8}$$

Finally, only initial conditions with zero total angular momentum L are considered,

$$L=\sum_n \det\begin{bmatrix} q_1 & q_2 & q_3 \\ p_1 & p_2 & p_3 \\ \hat{i} & \hat{j} & \hat{k} \end{bmatrix}_n =0. \tag{9}$$

Here $\hat{i}$, $\hat{j}$, and $\hat{k}$ are the Cartesian unit vectors, and of course $q_3=p_3=0\ \ \forall\ \ n$ by the above condition of planarity. The index n runs over the three particles. With the above restrictions, the relative orientation of three particles is specified with the space fixed confocal elliptic coordinates (ζ,η) to specify the position of the electron, and R to specify the relative internuclear distance.

For semiclassical quantization by the surface of section method, the following SOS figures were selected:

$$A_1=(p_\zeta,\zeta),\ \ \eta=\eta_c,\ \ R_c-\delta\leqslant R\leqslant R_c+\delta$$
$$A_2=(p_\eta,\eta),\ \ \zeta=\zeta_c,\ \ \ R_c-\delta\leqslant R\leqslant R_c+\delta \tag{10}$$
$$A_3=(p_R,R),\ \ \ (\zeta,\eta\ \text{unrestricted}).$$

The η_c and ζ_c are constants. Along any given trajectory the condition ($\eta=\eta_c$ and $R=$const) is met with vanishing frequency, so R is allowed to fall within a range $R_c-\delta\leqslant R\leqslant R_c+\delta$ in order to collect sufficiently many SOS points within a finite time. The width factor δ is chosen to be small enough that further reduction in δ results in no appreciable change in the area of the resulting SOS figure [13]. Empirically, $\delta=0.15$ bohr was found to meet this criteria. A typical (p_ζ,ζ) SOS figure is shown in Fig. 1. Note that $\zeta\geqslant 1$ in accordance with its definition (7), and the momentum p_ζ is small where ζ is maximum. The SOS areas were computed numerically by summation of the areas of an array of trapezoids, which were chosen to tile the SOS figure, a scheme that is equivalent to the common ''trapezoid rule'' for numerical integration. The uncertainty in the area computation was found to be $\pm 0.5\%$ with 100 SOS points defining the figure. Typically several hundred SOS points were used. As a check, selected areas were also computed with two other numerical methods. Tiling schemes based on circle sectors, and triangles both produced results in good accord with the trapezoidal rule integration.

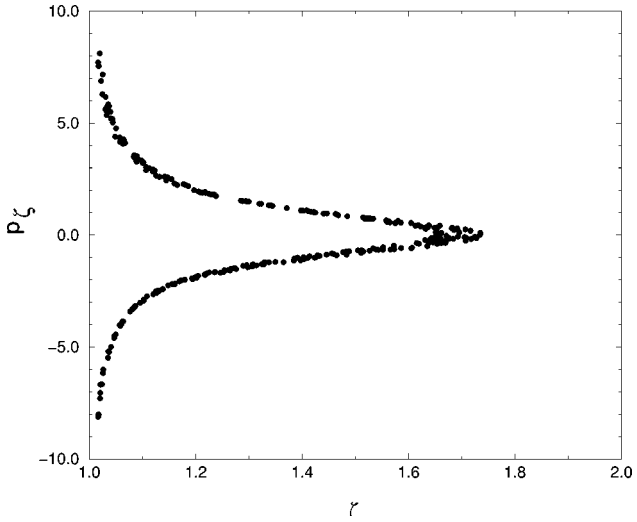

FIG. 1. Typical (p_ζ,ζ) SOS figure.

As suggested in Eq. (10), to compute A_3, (p_R,R) is simply accumulated for a few cycles of the nuclear motion with no restriction on ζ or η. The total energy is only weakly sensitive to A_3, so any error in the value of A_3 resulting from not restricting ζ and/or η introduces errors in the total energy far below those introduced by the uncertainty inherent in the calculation of A_1 (which is under full η and R restrictions) since the total energy is strongly dependent on A_1. An example (p_R,R) figure is shown in Fig. 2. The spikes result from the previously mentioned close electron-proton encounters.

In the limit $C\rightarrow 0$, ζ becomes a radius. A_1 therefore correlates with the action associated with radial motion in the united atom limit. For the σ^* state, discussed in Sec. III B, the total energy, by analogy to the hydrogen atom, depends

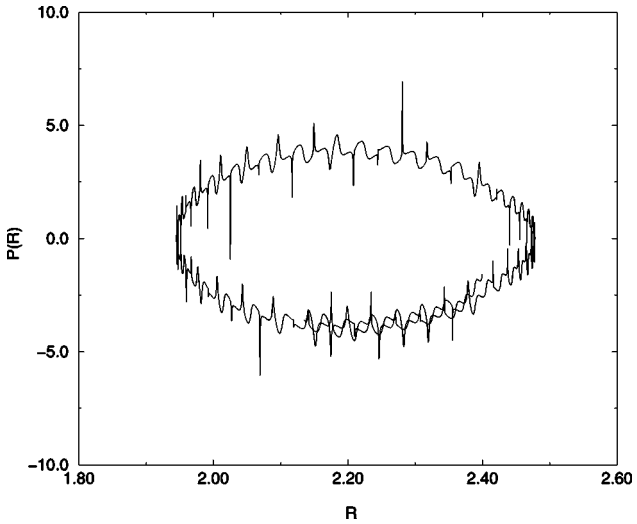

FIG. 2. (p_R,R) for about one cycle of the nuclear motion. Note the spikes that result from close electron-nucleus encounters (atomic units).

almost exclusively on A_1. This is the only action used in the semiclassical quantization of σ^* by the SOS method.

Since the numerical integration is accomplished in Cartesian coordinates and momenta, it is necessary to express the SOS coordinates (ζ,η,R) and their conjugate momenta (p_ζ,p_η,p_R) in terms of the Cartesian coordinates $\mathbf{q}_i$ and momenta $\mathbf{p}_i$, in order to generate the SOS figures from the trajectory data. The SOS coordinates are easily expressed in terms of the Cartesian coordinates by substitution of Eq. (5) into Eq. (7). To find expressions for the SOS momenta, we make use of

$$p_\zeta=\frac{\partial T}{\partial(d\zeta/dt)},$$

$$p_\eta=\frac{\partial T}{\partial(d\eta/dt)}, \tag{11}$$

$$p_R=\frac{\partial T}{\partial(dR/dt)},$$

where T is the kinetic energy operator

$$T=\frac{m_1\dot{\mathbf{q}}_1^2}{2}+\frac{m_2\dot{\mathbf{q}}_2^2}{2}+\frac{m_3\dot{\mathbf{q}}_3^2}{2}. \tag{12}$$

To find the SOS momenta based on Eq. (11) we need the kinetic energy operator T in terms of the SOS velocities, $\dot{\zeta}$, $\dot{\eta}$, $\dot{R}$. These velocities are given by

$$\dot{\zeta}=\frac{d\zeta}{dt}=\sum_\alpha\frac{\partial\zeta}{\partial q_\alpha}\dot{q}_\alpha,$$

$$\dot{\eta}=\frac{d\eta}{dt}=\sum_\alpha\frac{\partial\eta}{\partial q_\alpha}\dot{q}_\alpha, \tag{13}$$

$$\dot{R}=\frac{dR}{dt}=\sum_\alpha\frac{\partial R}{\partial q_\alpha}\dot{q}_\alpha.$$

Here the index α runs over the three spatial coordinates and each of the three particles. Equations (13) along with the constraints (8) and (9) result in the following system of six equations, which can be solved for the six nonzero Cartesian derivatives, $\dot{q}_\alpha$:

$$\begin{bmatrix} m_1 & 0 & m_2 & 0 & m_3 & 0 \\ 0 & m_1 & 0 & m_2 & 0 & m_3 \\ -m_1q_2 & m_1q_1 & -m_2q_5 & m_2q_4 & -m_3q_8 & m_3q_7 \\ \frac{\partial\zeta}{\partial q_1} & \frac{\partial\zeta}{\partial q_2} & \frac{\partial\zeta}{\partial q_4} & \frac{\partial\zeta}{\partial q_5} & \frac{\partial\zeta}{\partial q_7} & \frac{\partial\zeta}{\partial q_8} \\ \frac{\partial\eta}{\partial q_1} & \frac{\partial\eta}{\partial q_2} & \frac{\partial\eta}{\partial q_4} & \frac{\partial\eta}{\partial q_5} & \frac{\partial\eta}{\partial q_7} & \frac{\partial\eta}{\partial q_8} \\ \frac{\partial R}{\partial q_1} & \frac{\partial R}{\partial q_2} & \frac{\partial R}{\partial q_4} & \frac{\partial R}{\partial q_5} & \frac{\partial R}{\partial q_7} & \frac{\partial R}{\partial q_8} \end{bmatrix} \times \begin{bmatrix} \dot{q}_1 \\ \dot{q}_2 \\ \dot{q}_4 \\ \dot{q}_5 \\ \dot{q}_7 \\ \dot{q}_8 \end{bmatrix} = \begin{bmatrix} 0 \\ 0 \\ 0 \\ \dot{\zeta} \\ \dot{\eta} \\ \dot{R} \end{bmatrix}. \tag{14}$$

Here the subscript cycles over the three Cartesian spatial coordinates for each of the three particles, ($q_1=x_1$, $q_2=y_1$, $q_3=z_1$, $q_4=x_2,\ldots$). Note that the z components are all zero by the condition of planarity and therefore not present in Eq. (14). Substitution of the $\dot{q}_\alpha$ into Eq. (12) and subsequent differentiation according to Eq. (11) produces the required SOS momenta expressions, which for the sake of brevity are not reproduced here.

For semiclassical quantization, one could in principle search for initial conditions, which lead to a trajectory whose actions (SOS areas) satisfy the quantization condition. For multidimensional systems this involves searching over many initial conditions in an attempt to satisfy several quantization conditions simultaneously. In the present case, this demanding task is frustrated by a nonobvious mapping of initial conditions to actions. For multidimensional systems, a more efficient method of semiclassical quantization involves interpolating eigenenergies [33–35] based on an approximating function $E(A_1,A_2,\ldots,A_N)$. Using the methods outlined above, actions (SOS areas) were computed for many trajectories and the resulting energy vs actions data fit to the functional form

$$E(A_1,A_2,A_3)=c_1+c_2A_1+c_3A_2+c_4A_3+c_5A_1^2+c_6A_2^2+c_7A_3^2+c_8A_1A_2+c_9A_1A_3+c_{10}A_2A_3, \tag{15}$$

where the c_i were optimized by the method of least squares to give the best fit. Once the best fit is determined, the desired eigenenergy is easily computed. As an added advantage, this method allows the determination of primitive semiclassical eigenstates even in regions of phase space where the classical motion is chaotic [35]. There is one important caveat, this method works well only if the eigenstates are *interpolated* [35], a restriction that precludes the application of this technique to the higher vibrational levels of H_2^+ X $^2\Sigma_g$. With increasing energy, it becomes increasingly diffi-

TABLE I. Energetics for H_2^+ and D_2^+. Energies are relative to dissociation, i.e., $H(^2S) + H^+$ (in cm^{-1}). Note that in the clamped nuclei case [3] given in the column labeled SR, semiclassical H_2^+ $X\ ^2\Sigma_g(\nu=0)$ is unbound and only becomes bound when tunneling is included (uniform approximation). The present full three-body treatment predicts a weak chemical bond in the primitive semiclassical approximation. Of course there are no nuclear isotope effects in the clamped nuclei case because the nuclei are effectively infinite in mass. All values are in cm^{-1}.

State	SOS[a]	exact QM	SR[c]
$H_2^+ X^2\Sigma_g(\nu=0)$	-2.6×10^3	-21379.348[b]	$+724$ (-22694)
$D_2^+ X^2\Sigma_g(\nu=0)$	-2.7×10^3	-21711.580[b]	—
$H_2^+ \sigma^*$	$+2.9\times10^3$ (-9)[d]	-3.434[b]	—
$D_2^+ \sigma^*$	$+2.9\times10^3$ (-9)[d]	-5.513[b]	—

[a]Present work (uncertainty is ±20 in units of the last reported digit for $X\ ^2\Sigma_g$).
[b]Wolniewicz and Orlikowski [38].
[c]Strand and Reinhardt [3], primitive semiclassical, $H_2^+ X^2\Sigma$ (R = 2.0 bohr). The molecule is bound only in the uniform semiclassical approximation. (Value given parenthetically.)
[d]Uncertainty undetermined. Approximate primitive semiclassical energy by adiabatic switching given parenthetically.

cult to locate classical trajectories for which good actions can be computed. Only in the case of regular motion will the SOS points fall on a smooth curve [36], and the SOS figure have a well-defined area. While chaotic and autoionizing classical trajectories are both present in H_2^+ [37], our success lies in finding sufficiently many trajectories in the energy regime of interest for which smooth SOS figures (like that shown in Fig. 1) can be generated. Numerical trajectories do not reveal the ultimate fate of the system ($t\rightarrow\infty$), but the trajectories that were employed remained bound and regular for at least 1.25×10^4 atomic time units (about 0.3 ps).

In the present calculation there are issues of both accuracy and precision. The primitive semiclassical approximation is, of course, not equivalent to an exact solution to the Schrödinger equation but yields eigenstate energies that are only approximate. The difference between the primitive semiclassical result and the exact quantum result represents *methodological inaccuracy*. Generally the primitive semiclassical eigenenergy is above the corresponding exact quantum result because penetration of the quantum wave function into the classically forbidden region (an effect neglected in the primitive semiclassical case) permits more of phase space to be accessed by the wave function than is accounted for in the primitive semiclassical theory. As a consequence of this extra phase accumulation, quantizing eigenstates lie deeper in the potential and hence lower in energy than the semiclassical theory predicts. Nevertheless, the primitive semiclassical eigenenergy is a mathematically well-defined, albeit approximate, quantity. It is in obtaining this quantity that the issue of precision is encountered.

As discussed above, there is some uncertainty in computing the areas of the SOS figures. This uncertainty translates directly into uncertainty in the primitive semiclassical eigenenergy. In the present case, the uncertainty in the calculation of the areas of the SOS figures results in an uncertainty in the final eigenenergies of about ±2000 cm^{-1}. The cost of increasing this precision is not justified in light of the inaccuracy inherent in the primitive semiclassical approximation.

III. RESULTS AND DISCUSSION

A. The $X\ ^2\Sigma_g$ state

The state energies for H_2^+ as computed with the semiclassical SOS method but *without the Born-Oppenheimer approximation* (BO) are given in Table I, where a comparison is made to Strand and Reinhard's [3] semiclassical result (which includes the Born-Oppenheimer approximation) and to numerically exact quantum values [38]. Note in particular that while primitive semiclassical H_2^+ is unbound in the clamped nuclei (BO) approximation, when the full three-body dynamics is considered, H_2^+ is weakly bound within the primitive semiclassical approximation. A physical picture of this bonding is afforded by Fig. 3 which shows a portion of an electron trajectory that approximately corresponds to H_2^+ $X\ ^2\Sigma_g(\nu=0)$. A histogram of the electron's position is shown in Fig. 4. Note that the electron exchanges between the nuclei with its most probable position being between them. This is in accord with long standing views of chemical bonding. The remarkable observation is that this ''chemical bond,'' while very weak, is entirely classical. The electron's

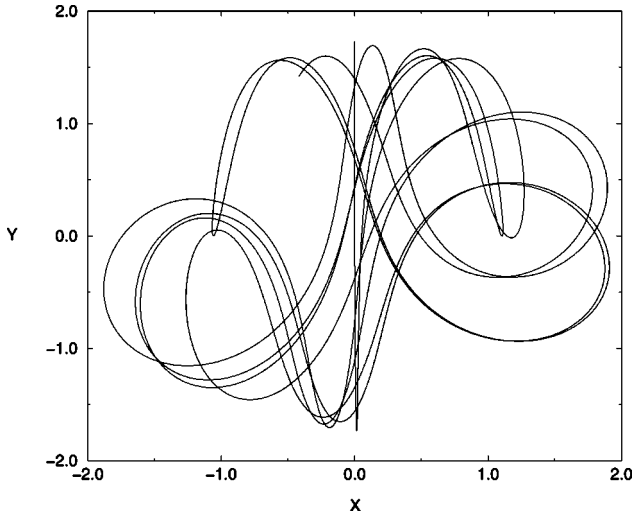

FIG. 3. A portion of an electron trajectory that approximately corresponds to H_2^+ $X\ ^2\Sigma_g(\nu=0)$ (atomic units).

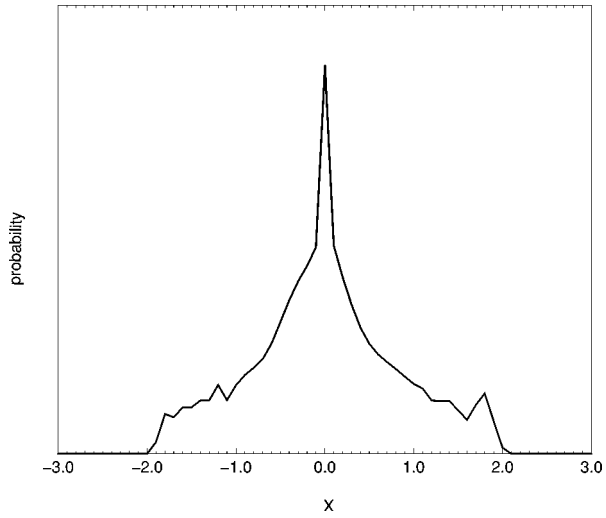

FIG. 4. Histogram of the electron's position for a trajectory that approximately corresponds to H_2^+ $X\ ^2\Sigma_g(\nu=0)$, which is shown in part in Fig. 3 (atomic units).

trajectory is found with Hamilton's classical mechanics, and the semiclassical quantization is primitive, making no adjustment for tunneling other than the standard $\pi/4$ phase accumulation at each turning point [8,9].

The exchange of the electron is most easily seen in Fig. 5, which shows the time dependence of the x component of the instantaneous molecular dipole. (The molecular axis is approximately parallel to the x axis.) Figure 5(a) is for a trajectory approximating H_2^+ $X\ ^2\Sigma_g(\nu=0)$, and Fig. 5(b) is for a trajectory approximating H_2^+ $X\ ^2\Sigma_g(\nu=1)$. Changes in sign of the x component of the instantaneous molecular dipole are a manifestation of the electron swapping nuclei. Note that the frequency of this exchange correlates with molecular vibration. Electron exchange or ''sharing'' is, of course, the signature of chemical bonding [1]. In Fig. 5 we clearly see the *classical* exchange of the electron between the nuclei.

B. The $^2\Sigma_u$ state (σ^*)

The $^2\Sigma_u$ state of H_2^+ nominally arises from the antisymmetric combination of the two hydrogenic $1s$ wave functions and in the treatment of Pauling [1] is antibonding, repulsive at all internuclear separations R. As first calculated by Peek [39], and much more recently observed for some H_2^+ isotopomers by Carrington *et al.* [40], this σ^* state has a weak van der Waals minimum at large R. It is easily shown that the classical exchange of the electron is forbidden in this σ^* state.

For the electron to exchange classically between the two nuclei it must at some time be exactly half-way between them, which represents the top of the potential barrier to exchange. This barrier decreases with decreasing R. The potential energy is

$$V(R)=\frac{1}{R}-\frac{1}{r_a}-\frac{1}{r_b}. \tag{16}$$

With the electron exactly half-way between the nuclei,

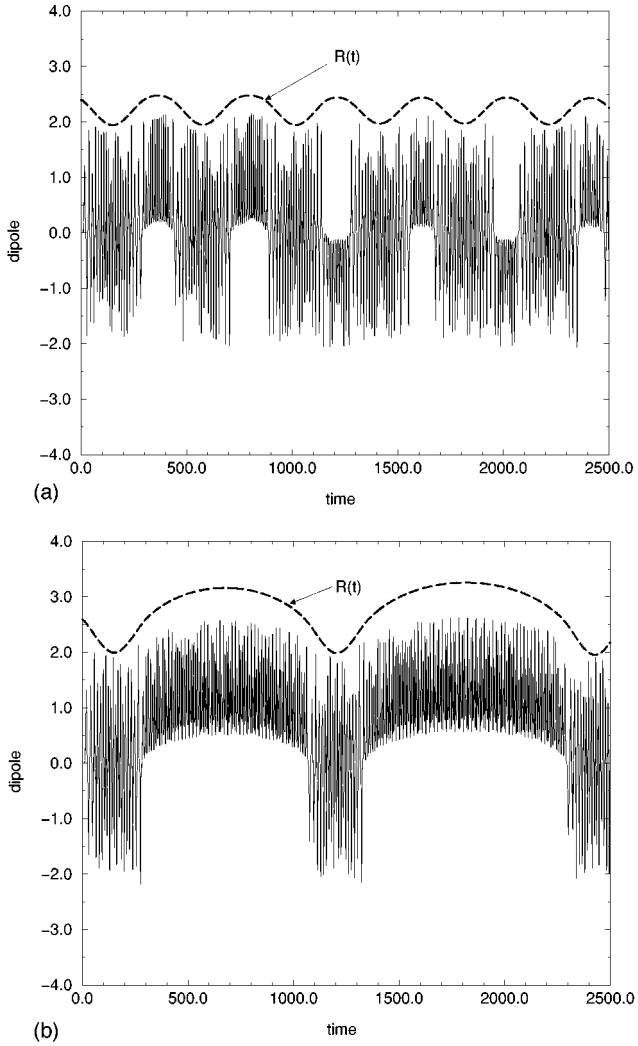

FIG. 5. Time dependence of the x component of the instantaneous molecular dipole. The time dependence of the internuclear separation R is superimposed (broken curve) for purposes of comparison. Note that classical electron exchange occurs only near the inner turning point. (a) H_2^+ $X\ ^2\Sigma_g(\nu=0)$. (b) H_2^+ $X\ ^2\Sigma_g(\nu=1)$. R in bohr, dipole in atomic units.

$$r_a=r_b=\frac{R}{2},$$
$$V(R)=\frac{-3}{R}. \tag{17}$$

According to Carrington *et al.* [40], the $\nu=0$ turning points on the σ^* PEC are $r_{\text{inner}}\approx 5$ Å$=9.45$ bohr, $r_{\text{outer}}\approx 10$ Å$=18.9$ bohr. At 9.45 bohr, the closest approach of the nuclei, the potential energy is $V(9.45)=-0.317$ hartree, which is the barrier to exchanging the electron. The σ^* state energies are [39] $D_2^+=-0.500025$ hartree, and $H_2^+=-0.5000156$ hartree. These energies are far below the height of the barrier to electron exchange. The electron can therefore only exchange between the nuclei by tunneling, a nonclassical process.

Note that since some energy is tied up in the kinetic energy of the electron, it is possible for the electron to be dynamically confined to one or the other nucleus, even

though its classical exchange is energetically allowed. Such a case is seen for the X $^2\Sigma_g$ state in Fig. 5 where the electron gets temporarily ''stuck'' on one nucleus even though R is such that classical electron exchange is energetically allowed. This effect betrays a total energy that is only slightly greater than the potential barrier to electron exchange, an energy regime where tunneling is particularly significant [41]. The close energetic proximity of the potential maximum to the eigenstate energies in H_2^+ accounts for the sizable tunneling correction [3].

Because the electron cannot exchange between the nuclei classically in the σ^* state, for primitive semiclassical quantization this state must be viewed as a perturbed hydrogen atom.

Consider the following physical picture: when a hydrogen atom is perturbed by bringing a second proton in from a great distance, the Coulomb potential well in which the electron is trapped expands slightly. Instead of rising symmetrically from $-\infty$ at the atomic center to the zero of potential far from the nucleus, in the direction of the perturbing proton the rise is slightly attenuated. This perturbation increases slightly the volume of the potential well and hence lowers the hydrogenic $1s$ eigenstate. Because the eigenstate in the perturbed system is slightly lower than that in separated $H + H^+$, the perturbed system is bound with respect to dissociation into a hydrogen atom plus a proton. The electron therefore orbits one nucleus with the second nucleus hovering at a greater distance.

The effect of the perturbing proton on the hydrogenic $1s$ eigenenergy is shown in Fig. 6, which displays the gradual transformation, H $1s \rightarrow$ H_2^+ σ^*. A classical trajectory is computed numerically such that at time $t=0$ the coordinates and momenta are set to mimic a hydrogen atom in the $1s$ state with a second bare proton placed at a distance equal to the nuclear separation at the outer classical turning point in H_2^+ $^2\Sigma_u(\nu=0)$. (As previously noted, the outer turning point is $R=18.9$ bohr [40].) The charge Q_1 on the bare proton, however, is given the time dependence

$$Q_1(t)=\frac{1}{1+e^{\beta(\phi-t)}}. \tag{18}$$

Here ϕ sets the switching time and β is chosen such that the rate of change of charge is very small, while still achieving the conditions $Q_1(0)\approx 0$ and $Q_1(2\phi)\approx 1$. Here $\beta=0.015$, $\phi=750$, and the final energy was found to be converged with respect to decreasing β. The time dependence of the charge Q_1 is also shown in Fig. 6. Clearly, the perturbing charge very slightly lowers the hydrogenic $1s$ eigenenergy.

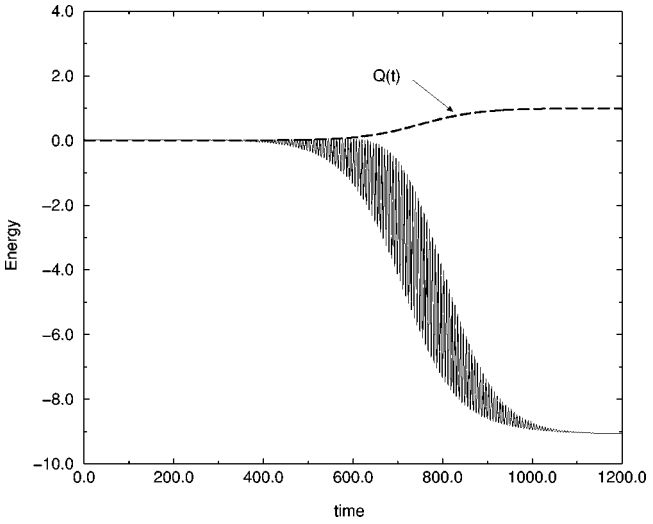

FIG. 6. Effect of a perturbing proton on the hydrogenic $1s$ eigenenergy. The solid curve shows the system energy (in cm^{-1}) as a function of time over the course of a numerical classical trajectory whose initial conditions mimic a hydrogen atom in its $1s$ eigenstate. The broken curve shows the time dependence of the charge on a bare proton placed at a distance equal to the separation of the nuclei at the outer classical turning point in H_2^+ $^2\Sigma_u(\nu=0)$.

IV. SUMMARY

The extension of the surface-of-section method of primitive semiclassical quantization to a three-body [42], three-mode system has permitted the semiclassical quantization of the hydrogen molecular ion H_2^+ without the restriction of the Born-Oppenheimer separation of nuclear and electronic motions. Unlike the clamped-nuclei approximation, in the present full three-body treatment, primitive semiclassical quantization properly predicts the sign of the dissociation energy of H_2^+. While primitive semiclassical quantization gives a quantitatively inaccurate description of the one-electron chemical bond in H_2^+ because it ignores the dominant tunneling contribution, it does reveal a previously unappreciated 10% classical contribution.

The σ^* van der Waals state of H_2^+ is also discussed and shown to correspond physically to a perturbed hydrogen atom. The slight expansion of the Coulomb potential well brought about by an adjacent proton leads to a bound H_2^+ state by lowering very slightly the $1s$ hydrogen ground-state level.

ACKNOWLEDGMENTS

This work was sponsored by the Division of Materials Sciences, Office of Basic Energy Sciences, U.S. Department of Energy under Contract No. DE-AC05-96OR22464 with Lockheed-Martain Energy Research Corporation. K.S. thanks Professor R. B. Shirts for useful discussions and Professor K. Szalewicz for the use of his computing resources.

[1] L. Pauling, Chem. Rev. **5**, 173 (1928).
[2] L. Pauling, *The Nature of the Chemical Bond* (Cornell University Press, Ithaca, NY, 1960).
[3] M. P. Strand and W. P. Reinhardt, J. Chem. Phys. **70**, 3812 (1979).
[4] F. Luo, C. McBane, G. Kim, C. F. Giese, and W. R. Gentry, J. Chem. Phys. **98**, 3564 (1993); F. Luo, C. McBane, G. Kim, C. F. Giese, and W. R. Gentry *ibid.* **100**, 4023 (1994); W. Schöllkopf and J. P. Toennies *ibid.* **104**, 1155 (1196).
[5] A. R. Janzen and R. A. Aziz, J. Chem. Phys. **107**, 914 (1997); T. Korona, H. L. Williams, R. Bukowski, B. Jeziorski, and K. Szalewicz, *ibid.* **106**, 5109 (1997); for a qualitative discussion, see also S. Borman Chem. Eng. News, Feb. 22, 26 (1993).
[6] J. Müller, J. Burgdörfer, and D. W. Noid, J. Chem. Phys. **103**, 4985 (1995).
[7] C. Marchal, *The Three Body Problem* (Elsevier, Amsterdam, 1990).
[8] D. Bohm, *Quantum Theory* (Dover, New York, 1989), is an excellent reference for both WKB and the old quantum theory.
[9] J. B. Keller, Ann. Phys. (N.Y.) **4**, 180 (1958).
[10] R. A. Marcus, Discuss. Faraday Soc. **55**, 34 (1973).
[11] D. W. Noid and R. A. Marcus, J. Chem. Phys. **62**, 2119 (1975).
[12] D. W. Noid and R. A. Marcus, J. Chem. Phys. **67**, 559 (1977).
[13] D. W. Noid, M. L. Koszykowski, and R. A. Marcus, J. Chem. Phys. **73**, 391 (1980).
[14] D. W. Noid and B. G. Sumpter, Chem. Phys. Lett. **121**, 187 (1985); S. K. Knudson and D. W. Noid *ibid.* **145**, 16 (1987).
[15] M. C. Gutzwiller, J. Math. Phys. **12**, 343 (1971); M. C. Gutzwiller, J. Phys. Chem. **92**, 3154 (1988).
[16] W. H. Miller, Faraday Discuss. Chem. Soc. **62**, 40 (1977); W. H. Miller, J. Chem. Phys. **63**, 996 (1975).
[17] M. V. Berry and M. Tabor, Proc. R. Soc. London, Ser. A **349**, 101 (1976).
[18] I. C. Percival, J. Phys. A **7**, 794 (1974).
[19] C. C. Martens and G. S. Ezra, J. Chem. Phys. **83**, 2990 (1985); C. C. Martens and G. S. Ezra *ibid.* **86**, 279 (1987).
[20] C. W. Eaker and G. C. Schatz, J. Chem. Phys. **81**, 2394 (1984); C. W. Eaker, G. C. Schatz, N. DeLeon, and E. J. Heller, J. Chem. Phys. **81**, 5913 (1984).
[21] G. C. Schatz, Comput. Phys. Commun. **51**, 135 (1988).
[22] T. J. Pickett and R. B. Shirts, J. Chem. Phys. **94**, 6036 (1991).
[23] For a review of the adiabatic switching method and numerous applications, see R. Skodje and J. R. Cary, Comput. Phys. Rep. **8**, 221 (1988).
[24] V. I. Arnold, *Mathematical Methods of Classical Mechanics* (Springer, New York, 1980).
[25] F. G. Gustavson, Astron. J. **71**, 670 (1966).
[26] J. B. Delos and R. T. Swimm, Chem. Phys. Lett. **47**, 76 (1977); R. T. Swimm and J. B. Delos, J. Chem. Phys. **71**, 1706 (1979).
[27] C. Jaffé and W. P. Reinhardt, J. Chem. Phys. **77**, 5191 (1982).
[28] R. B. Shirts and W. P. Reinhardt, J. Chem. Phys. **77**, 5204 (1982).
[29] K. Sohlberg and R. B. Shirts, Phys. Rev. A **54**, 416 (1996).
[30] L. F. Shampine and M. K. Gordon, *Computer Solution of Ordinary Differential Equations: The Initial Value Problem* (Freeman, San Francisco, 1975).
[31] All calculations were performed on a 195 MHZ SGI Indigo2 Power Challenge R10000 with 128MB main RAM.
[32] A. M. Hiltebietel, Am. J. Math. **33**, 337 (1911).
[33] B. G. Sumpter and D. W. Noid, Chem. Phys. Lett. **126**, 181 (1986).
[34] R. Ramaswamy, J. Chem. Phys. **82**, 747 (1985).
[35] K. Sohlberg and R. B. Shirts, J. Chem. Phys. **101**, 7763 (1994).
[36] M. Hénon and C. Heiles, Astron. J. **69**, 73 (1964).
[37] J. H. VanVleck, Bull. Nat. Res. Council, **54** (1926) Chap. VII.
[38] L. Wolniewicz and T. Orlikowski, Mol. Phys. **74**, 103 (1991); L. Wolniewicz and J. D. Poll, *ibid.* **59**, 953 (1986).
[39] J. M. Peek, J. Chem. Phys. **50**, 4595 (1969).
[40] A. Carrington, C. A. Leach, A. J. Marr, R. E. Moss, C. H. Pyne, and T. C. Steimle, J. Chem. Phys. **98**, 5290 (1993); A. Carrington, I. R. McNab, C. A. Montgomerie, and R. A. Kennedy, Mol. Phys. **67**, 711 (1989).
[41] R. Paulsson, F. Karlsson, and R. J. Le Roy, J. Chem. Phys. **79**, 4346 (1983).
[42] J. Müller, J. Burgdörfer, and D. W. Noid, Phys. Rev. A **45**, 1471 (1992).